Synergistic flame retardant effect of melamine in ethylene–vinyl acetate/layered double hydroxides composites

Long Li · Yi Qian · Chuanmei M. Jiao

Abstract Mg–Al–Fe ternary layered double hydroxides (LDHs) were synthesized based on Bayer red mud by a calcination–rehydration method, and characterized by X-ray diffraction (XRD) and thermogravimetric analysis (TG). The synergistic effects between melamine and LDHs in ethylene–vinyl acetate (EVA) composites were studied using limiting oxygen index (LOI), UL 94, cone calorimeter test (CCT), smoke density test (SDT), and thermogravimetry–fourier transform infrared spectrometry (TG–IR). Though melamine decreases the LOI values of EVA/LDHs/melamine composites, a suitable amount of melamine can apparently improve UL 94 rating; the composite with 45 % LDHs and 5 % melamine can pass UL 94 test. The CCTs results indicate that heat release rates (HRR) of EVA/LDHs/melamine composites decreased in comparison with that of EVA/LDHs composites. The SDT results show that melamine is helpful to smoke suppression. The TG–IR data show that the ternary composites have a higher thermal stability than that of the binary composites.

Keywords Flame retardant · Melamine · Layered double hydroxides · Bayer red mud · Synergisctic effects

Introduction

Ethylene–vinyl acetate (EVA) copolymers with different acetate contents are extensively used in many fields,

L. Li · Y. Qian (✉) · C. M. Jiao
College of Environment and Safety Engineering,
Qingdao University of Science and Technology, Qingdao,
Shandong 266042, People's Republic of China
e-mail: qianyi1962@126.com

especially in the cable industry as excellent insulating materials with good physical and mechanical properties [1]. However, EVA copolymers are particularly flammable and emit a large amount of smoke when burning, which restricts their practical applications [2]. Therefore, it is very important to improve the flame retardance in the applications of EVA materials.

Layered double hydroxides (LDHs), as an environmentally friendly halogen-free flame retardant additives, have been extensively used in the flame retardation of polymers; because of their advantages such as low smoke, no toxicity, and no corrosive gas generation [3]. However, LDHs has an essential disadvantage that more than 60 % loading in the polymer blends is required to obtain an adequate level of flame retardant properties, which could be detrimental to the mechanical properties of flame retardant polymer materials [4], because of the poor compatibility between inorganic additives and polymer resin [5]. In order to improve the mechanical properties of flame retardant composites, surface treatment of LDHs by coupling agents has been widely used to improve their compatibility [2, 6]. However, this kind of improvement of mechanical properties is not only very limited, but also this surface modification brings the deterioration of flame retardant properties, because most of organic coupling agents are flammable [7]. Many studies show that the synergistic effects of some halogen-free flame retardant agents (such as ammonium polyphosphate [8–10], hyperfine magnesium hydroxide [6, 11], and red phosphorus [12]) with LDHs can enhance flame retardancy and reduce the high loading level of LDHs, thus improving the mechanical properties of the flame retardant materials.

Melamine is usually used as the gas generated source of an intumescent flame retardant system. Many works have been done about its synergistic effects with other flame

retardants [13–16]. Melamine can release nitrogen and ammonia to dilute the oxygen and flammable gas when heated. At the same time, it can accelerate the carbonation of the polymers to form a char layer on the surface of the matrix. As far as we are aware, few works have been done on the synergistic effect of melamine with LDHs in EVA/LDHs composites.

Bayer red mud is one typical kind of red mud which is formed in the production of alumina by leaching the bauxite in the alkali. Bayer red mud containing lots of Al and Fe elements could be used to prepare the LDHs [17]. Though the reports about synthesis of LDHs are a lot, but few have used an industrial waste such as Bayer red mud as raw material. In this paper, Mg/Al/Fe–CO_3 LDHs were synthesized and characterized by X-ray diffraction (XRD) and thermogravimetric analysis (TG). Moreover, the synergistic effects of LDHs with melamine have been studied using limiting oxygen index (LOI), UL 94 test, cone calorimeter (CCT), smoke density test (SDT), and thermogravimetry–fourier transform infrared spectrometry (TG–IR).

Experimental

Materials

EVA18 (containing 18 wt% vinyl acetate) was bought from Beijing Eastern Petrochemical Co., Ltd. (China). Bayer red mud was kindly supplied by Aluminum Corporation of China Shandong Branch. It contains O (37.12 %), Na (7.11 %), Al (11.33 %), Si (5.16 %), S (0.4 %), Ca (0.62 %), Ti (2.15 %), Fe (35.61 %), and Co (0.5 %) (The result is examined by an INCA Energy X-ray energy spectrometer (EDS, Oxford) after roasted at a temperature of 650 °C for 4 h). Melamine was bought from Sinopharm Chemical Reagent Co., Ltd. (China). Other reagents were the standard laboratory reagents, and used as received without further purification.

Sample preparation

Synthesis of LDHs

Bayer red mud is dried at a temperature of 100 °C for 4 h, and is grinded by a Ball Machine into 300-mesh-pass particles. Then, Bayer red mud and MgO are mixed with Mg/(Al+Fe) molar ratios of 4.0/1.0. The mixture is roasted at a temperature of 650 °C for 4 h used a muffle furnace, then the roasted mixture is leaching in Na_2CO_3 solution with $[CO_3^{2-}]/([Al^{3+}]+[Fe^{3+}]) = 2.0$. Each mixed process is simultaneously added to an emulsifying machine with a rotor speed of 200 r min^{-1} and mixed for 10 h. Then, the slurry is filtered, washed thoroughly, and dried at 100 °C for 24 h to obtain Mg/Al/Fe–CO_3 LDHs. At last, the Mg/Al/Fe–CO_3 LDHs was grinded into 300-mesh-pass particles (with a particle size of about 48 μm) as flame retardants.

Preparation of the EVA composites

All compositions were melt-compounded with a mixer at 120 °C for 10 min. After mixing, the mixtures were compression-molded into sheets at 120 °C under a pressure of 10 MPa for 10 min. Then, the sheets were cut into suitable size for fire testing. The formulations are given in Table 1.

Measurements

X-ray diffraction (XRD)

XRD was carried out at room temperature on a Philips X'Pert Pro Super apparatus (Nicolet Instrument Co., Madison, WI) using Cu Ka radiation with a nickel filter (wavelength = 1.5418 Å) at a scan rate of 0.0167 s^{-1}.

Thermogravimetry–fourier transform infrared spectrometry

The TG–IR instrument consists of a thermogravimeter (TG209 F1, Netzsch Instruments, Germany), a fourier transform infrared spectrometer (Vertex70, Bruker Optics, Germany), and a transfer tube with an inner diameter of 1 mm connected to the TG and the infrared cell. The investigation was carried out from 30 to 900 °C at a linear heating rate of 20 °C min^{-1} under a nitrogen flow of 30 mL min^{-1}. The FTIR was not used when the TG behavior of the Mg/Al/Fe–CO_3 LDHs was tested.

Limiting oxygen index

LOI was measured according to ASTM D 2863. The apparatus used was an HC-2 oxygen index meter (Jiangning Analysis Instrument Company, China). The specimens used for the test were of dimensions 100 × 6.5 × 3 mm^3. At least five specimens were tested in each experiment.

UL 94 test

The UL 94 test was carried out on a CFZ-2-type instrument (Jiangning Analysis Instrument Company, China) according to the ASTM D 3801 testing procedure. The specimens used were of dimensions 100 × 13.0 × 3 mm^3. At least five specimens were tested in each experiment.

Table 1 LOI values and UL 94 test results for EVA/LDHs/melamine composites

Sample code	EVA/ %	LDHs/ %	Melamine/ %	LOI/ %	UL 94 rating	Phenomenon
EVA	100	0	0	17.0	Fail	Dripping
ELDH1	50	50	0	26.8	V-1	Dripping
ELDH2	50	49	1	26.7	Fail	Dripping
ELDH3	50	47	3	26.6	Fail	Dripping
ELDH4	50	45	5	25.6	V-0	No dripping
ELDH5	50	43	7	25.2	Fail	No dripping
ELDH6	50	41	9	25.1	Fail	No dripping
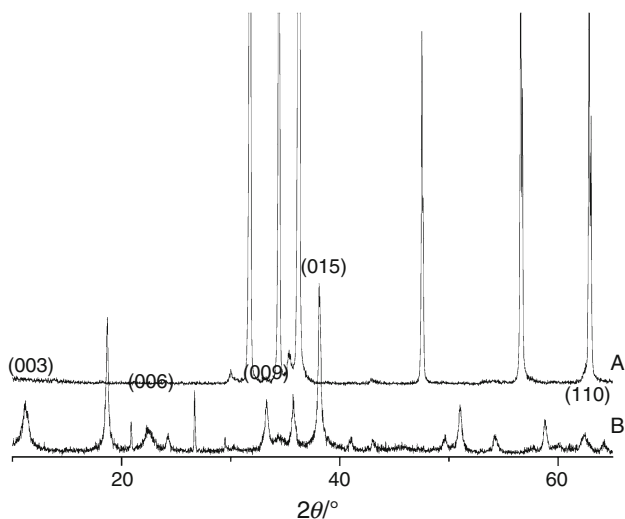
Fig. 1 XRD patterns of **a** Bayer red mud and **b** Mg/Al/Fe–CO3 LDHs

Cone calorimeter test (CCT)

The cone calorimeter (Stanton Redcroft, UK) test was performed according to the ISO 5660 standard procedures. Each specimen of dimensions $100 \times 100 \times 4 \ mm^3$ was wrapped in aluminum foil and exposed horizontally to an external heat flux of 50 kW m^{-2}. At least three specimens were needed in each experiment.

Smoke density test (SDT)

A Smoke density test machine JQMY-2 (Jianqiao Co, China) was used to measure the smoke characteristics according to ISO 5659-2(2006). Each specimen of dimensions $75 \times 75 \times 2.5 \ mm^3$ was wrapped in aluminum foil and exposed horizontally to an external heat flux of 25 kW m^{-2} with or without the application of a pilot flame.

Results and discussion

Characterization of the Mg/Al/Fe–CO3 LDHs

XRD characterization of the Mg/Al/Fe–CO3 LDHs

XRD patterns of the Mg/Al/Fe–CO3 LDHs and Bayer red mud are shown in Fig. 1. The (003), (006), (009), (110), and (115) diffraction peaks of Mg/Al/Fe–CO3 LDHs are in good agreement with layered structures, and ascribable to LDHs indexed in a hexagonal lattice. While the XRD pattern of Bayer red mud does not show the same peaks. The sharp diffraction peaks and the low baselines indicate relatively well-formed crystalline layered structures of Mg/Al/Fe–CO3 LDHs [18]. It can be concluded that when a suitable amount of Mg element is introduced into the Bayer red mud, LDHs can be synthesized successfully.

TG behavior of the Mg/Al/Fe–CO3 LDHs

Figure 2 presents TG and differential thermogravimetry (DTG) curves of Mg/Al/Fe–CO3 LDHs and Bayer red mud. From Fig. 2, it can be seen that all the samples exhibit a two-step mass-loss process. The first step of Mg/Al/Fe–CO3 LDHs below 250 °C is attributed to the loss of loosely bound water in the interlayer space; the maximum decreasing rates of mass-loss (T_{max}) at this step are 100.2 °C. The second step starts above 250 °C, which belongs to the simultaneous dehydroxylation of the lattice; T_{max} at this step is 391.5 °C [19]. The first step of Bayer red mud appears below 200 °C; the maximum decreasing rates of mass-loss (T_{max}) at this step are 93.8 °C. The second step starts above 200 °C, and the T_{max} at this step is 283.4 °C. It can be seen that Mg/Al/Fe–CO3 LDHs shows higher decomposition rate and T_{max} than the Bayer red mud. Moreover, above 700 °C, the amount of residue left after the degradation is different for the two samples, Bayer red left more residue than LDHs obviously. This may be illustrated by the interlayer structure of the LDHs, which could load more water than the Bayer red mud.

Flame retardant properties of the EVA/LDHs/melamine composites

LOI values and UL 94 rating of the EVA/LDHs/melamine composites

The LOI and UL 94 test are widely used to evaluate flame retardant properties of materials and to screen flame retardant formulations [20]. Table 1 presents the LOI values and UL 94 test results of the flame retardant EVA/LDHs/melamine composites. From Table 1, it can be seen that the LOI value of ELDH1 with only 50 % LDHs
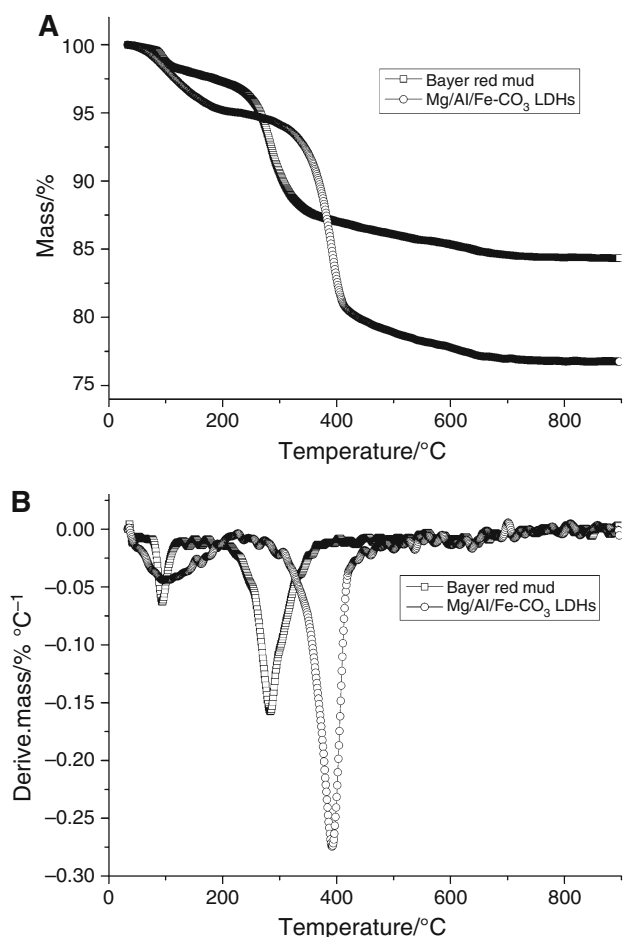
Fig. 2 TG and DTG *curves* of the LDHs and Bayer red mud

increases rapidly from 17.0 to 26.8 % of the pure EVA. Then the LOI values of the composites (ELDH2–ELDH6) decreases slightly to 25.1 % with increasing of melamine in the formulation. This phenomenon could be explained by the fact that there is a decrease in the loading of LDHs. When the flame retardant samples are heated, LDHs decompose to form water, diluting the flammable gases and oxygen, and decreasing the temperature, which is helpful to LOI test.

The UL 94 results showed that the EVA/LDHs/melamine composites with 5 % melamine can pass the UL 94 test. The samples (EVA and ELDH1–ELDH3) without melamine drip greatly in the UL 94 test, while the samples (ELDH4–ELDH6) with melamine do not show dripping phenomena in the process of the UL 94 test. This may be that some viscous materials generated in the decomposition of melamine favor the UL 94 test.
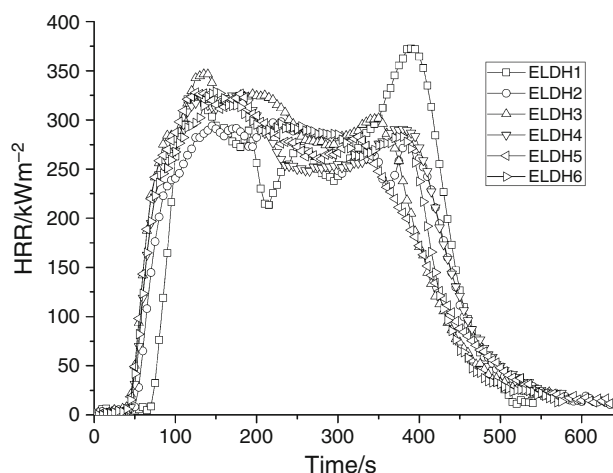
CCT of the EVA/LDHs/melamine composites

HRR of the EVA/LDHs/melamine composites The fire performances of flame retardant EVA/LDHs/melamine

composites were tested using cone calorimeter. The HRR curves of the EVA/LDHs/melamine composites with different loading of melamine are shown in Fig. 3; the correlated data are listed in Table 2.

The heat release rate (HRR) measured by cone calorimeter is a very important parameter as it expresses the intensity of a fire, which in turn determines other parameters. The pk–HRR (PHRR) value is used to express the intensity of a fire [21–23]. It can be found from Fig. 3 that the HRR curves of ELDH2–ELDH6 are all declined, and the combustion are all prolonged slightly by the addition of melamine compared with that of the ELDH1. For ELDH2–ELDH6, with the increase of melamine, HRR first decreases, then increases slightly; the HRR of ELDH4 (with a PHRR of 325.4 kW m^{-2}) is the lowest among all samples. It should also be figured out that the time to ignition and flame out show the same trends with HRR for ELDH2–ELDH6. ELDH4 takes more time to be ignited than the other composites; its combustion time is prolonged to 523 s. These phenomena indicate that an appropriate amount of melamine is needed for the improvement of the flame retardancy. Unfortunately, when melamine is added into the composites, the time to ignition of sample ELDH2–ELDH6 is shorter than that of ELDH1, because of the decrease of the decomposition of EVA catalyzing by LDHs.
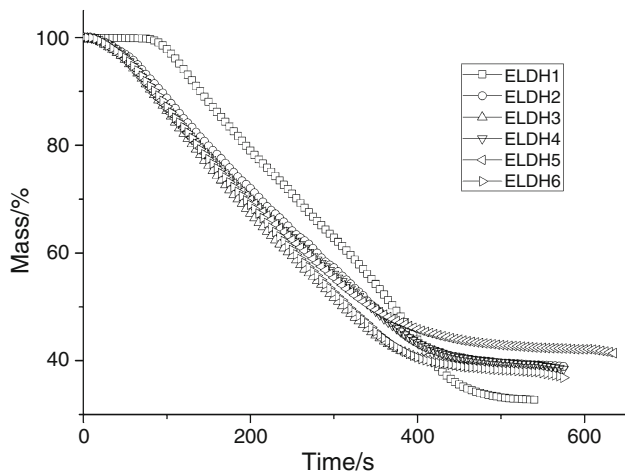
It is interesting to find that the first PHRR of the flame retardant samples (ELDH2–ELDH6) does not decrease with the increase of melamine, while the last PHRR of the flame retardant decreases apparently. The reason may be that the char residue could separate the internal material with the external oxygen and heat cannot be formed in a short time [15, 16]. We also notice separate multiple peaks in the HRR curves which reflect the gradual burning of the specimen through the thickness after the initial charred layers are formed. This combustion feature of multiple

Fig. 3 HRR of the EVA/LDHs/melamine composites

Table 2 The Data from cone calorimeter test

Sample code	PHRR/ $kW\ m^{-2}$	Time to ignition/s	Time to PHRR/s	Time to flame out/s
ELDH1	372.4	51	390	465
ELDH2	328.7	34	165	467
ELDH3	325.4	37	195	509
ELDH4	298.2	46	245	523
ELDH5	327.7	34	140	520
ELDH6	346.5	35	150	479

Fig. 4 The mass of the EVA/LDHs/melamine composites

HRR peaks has also been reported by Grexa and Fu [24, 25].

Mass of the EVA/LDHs/melamine composites Figure 4 shows the mass of the char residues. During combustion, a compact char may occur on the surface of material, creating a physical protective barrier. The char would act as a protective barrier in addition to the compact shield, and can thus limit the oxygen diffusion into the substrate, or give a less disturbing low volatilization rate. The char can also prevent the heat mass transfer between the flame zone and the burning substrate, and thus protect the underlying materials from further burning and retard the pyrolysis of polymers [2–4]. In this study, the compact char residue of ELDH2–ELDH6 formed on the surface of the sample, as shown in Fig. 5.

Digital photos of residues Figure 5 are digital photos of residues of EVA/LDHs/melamine composites. It can be seen that the residue of sample ELDH1 without melamine is very loose. However, a coherent residue can be formed on the surface of the samples with melamine. It is obvious that ELDH4 has a compact char layer to prevent the underline matrix from further burning, which may be the

main reason for its good performance in UL 94 test. From the char structure, we can explain the combustion phenomenon of the flame retardant EVA composites, which correlates well with the CCT results.

SDT of the EVA/LDHs/melamine composites

While the cone calorimeter results reflect the combustion behavior of the samples, the smoke density test gives a more detail information about the smoke production.

Specific optical density (SOD) can be used to evaluate the amount of smoke production. From Fig. 6, it can be seen that ELDH2–ELDH6 produce more smoke than sample ELDH1 before 600 s whether the pilot flame is or not used in the test; when the time exceeds 600 s, they produce less smoke than ELDH1. The reason for these phenomena may be that LDHs is more helpful to smoke suppression than melamine; Because of the CO_3^{2-} in its layer structure in the first 600 s. After that, melamine can work together with LDHs to form a char layer, which covered on the surface of the matrix, decreasing the smoke production. It is obvious that with the increase of melamine in EVA/LDHs/melamine composites, the smoke suppression character of the materials is improved at initial, and then becomes worse. ELDH4 shows the best smoke suppression performance among all samples, which is in good agreement with the CCT results. Moreover, when the pilot flame is used, the amount of smoke production is reduced than that without the pilot flame. The reason may be that when the pilot flame is used, the solid particles formed from the depolymerization of the polymers are mainly burned out to form gases, but do not migrate directly into the gas phase to increase the amount of smoke [26].

The SDT results showed that there are synergistic effects between melamine and LDHs in smoke suppression when the composites are exposed to heat. This can be explained by the decomposition of melamine and LDHs, and the formation of a char layer. On one hand, melamine and LDHs can release gas such as N_2, NH_3, H_2O, and CO_2 to dilute the smoke; on the other hand, both of them can accelerate the carbonization of the EVA, and work together to form a char layer. Thus, combustion products such as tar and soot particles are limited in making the transition to the gas phase, and so the smoke density can be effectively reduced [27].

TG–IR characterization of the EVA/LDHs/melamine composites

TG behavior of the EVA/LDHs/melamine composites

TG–IR analysis is always used to study the thermal degradation behavior of flame retardant materials; it also enables us to analyze the changes in evolved gases at

Fig. 5 *Photographs* after cone calorimeter test: **a** ELDH1, **b** ELDH2, **c** ELDH3, **d** ELDH4, **e** ELDH5, and **f** ELDH6
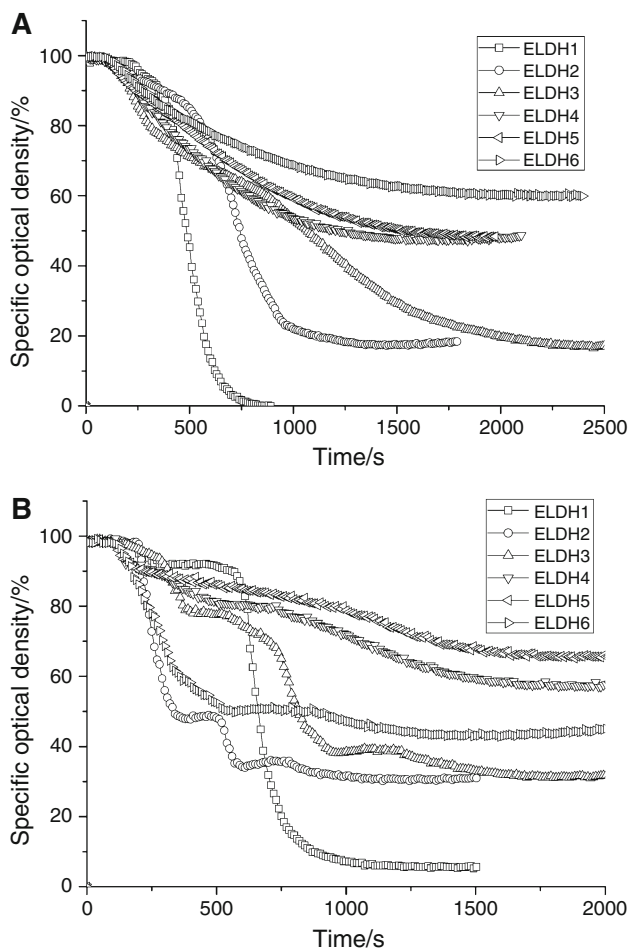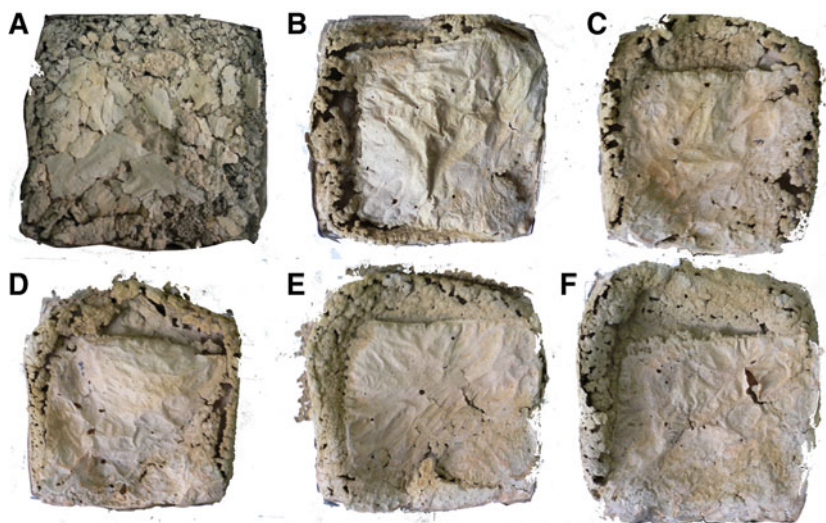

Fig. 6 SOD of the EVA/LDHs/melamine composites: **a** without the application of a pilot flame, and **b** with the application of a pilot flame

various temperatures [28, 29]. Figure 7 shows the TG curves of samples EVA, ELDH1, and ELDH4 in nitrogen atmosphere.

The thermal stability of a polymeric material is extremely important when it comes to a flame retardant, which is mainly concerned about the release of decomposition products and the formation of char [10]. It can be seen that EVA undergoes two degradation steps as shown in Fig. 7. The first decomposition step is due to the loss of carboxylic acid; the second involves random chain scission of the remaining material, forming unsaturated vapor species, such as butane and ethylene [30, 31]. ELDH1 and ELDH4 show three mass-loss steps. The first step of the composites is attributed to the loss of loosely bound water in the interlayer space of LDHs in the composites. The second and the third steps belong to the simultaneous dehydroxylation and decarbonization of the lattice of LDHs, which overlap with the decomposition of the acetate groups in EVA side chains and the scission of the main chains of EVA [19, 30].

It can also be noticed that ELDH1 shows lower decomposition rate in the third step, but higher decomposition rate in the first and the second step than EVA. The incorporation of LDHs lowers the decomposition rate of the third step, but accelerates the loss of carboxylic acid. It is obvious that the −OH groups on the fillers can assist β-hydrogen leaving. That is to say that the loss of carboxylic acid, which can be catalyzed by LDHs. This has been also reported by M. Zanetti and V.G. Gregoriou [31, 32]. At the temperature above 700 °C, EVA can leave nothing, while both ELDH1 and ELDH4 can leave 35 %. Moreover, the ternary composites ELDH4 with both melamine and LDHs show lower thermal stability at about 400 °C, but higher thermal stability in the other temperatures than the ELDH1. This should be the main reason that the ternary composites have better flame retardant effects than EVA/LDHs composites have. This result confirms the synergistic effects between melamine and LDHs. From the TG behavior of the ELDH1 and ELDH4, it is interesting to find
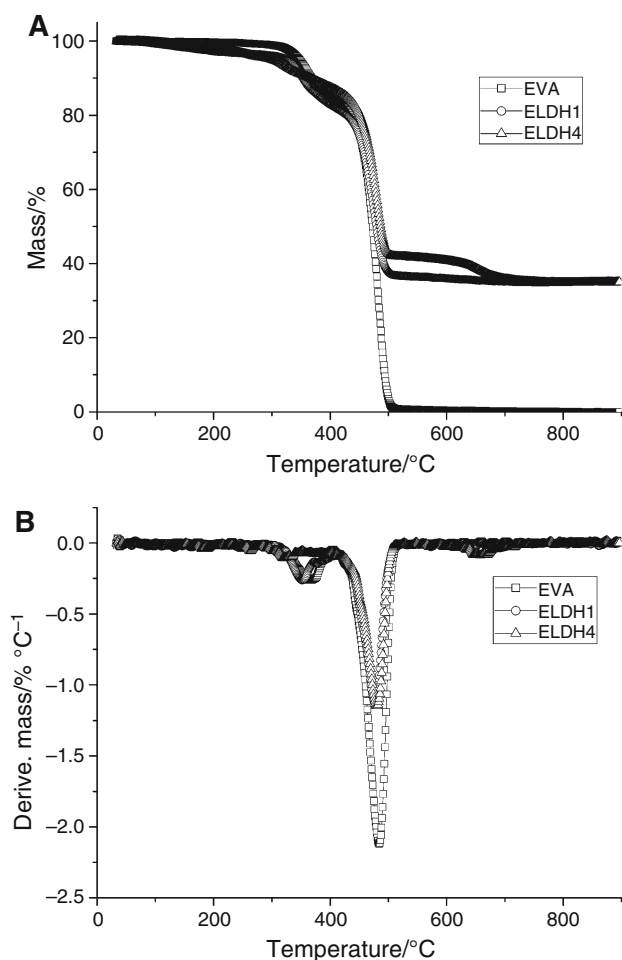
Fig. 7 TG and DTG *curves* of EVA, ELDH1, and ELDH4 composites

that an effective flame retardant performance needs the improvement of the char morphology, not the increase of the char yield. The same conclusion can be found in Weil and Pate's study [33].

## FTIR characterization of the EVA/LDHs/melamine composites

Figure 8 shows the 3D TG–IR spectra of pyrolysis products of the composites during the thermal degradation. From Fig. 8, It can be seen that the evolved gas products of the three samples exhibit characteristic bands of 3,400–4,000, 2,800–3,150, 2,250–2,400, 1,700–1,850, 1,250–1,500, and 950–1,150 cm^{-1}. The spectra fit well with the reported FTIR features of gas products such as H_2O (3,400–4,000 cm^{-1}), CO_2 (2,300–2,400 cm^{-1}), CO (2,250–2,300 cm^{-1}), carboxylic acid (1,700–1,850 cm^{-1}), and aliphatic hydrocarbons (2,800–3,150, 1,250–1,500, and 950–1,150 cm^{-1}) [34–36]. In this study, the main decomposition products of the composites are CO, CO_2, H_2O, carboxylic acid, and aliphatic hydrocarbons.

From the different pyrolysis products from the composites during the thermal degradation, it can be noticed that the degradation processes of the three samples are significantly different. Pure EVA decomposes dramatically when heated, and produces lots of carboxylic acid and aliphatic hydrocarbons. It is obvious that the decomposition of ELDH1 containing LDHs is slowed down. However, the decomposition of ELDH4 with melamine is accelerated slightly than ELDH1. The reason for this phenomenon may be that melamine is not so stable as LDHs when heated, and the amount of LDHs is decreased when it is partly substituted by melamine.

The characteristic spectra obtained from 30 to 900 °C are shown in Fig. 9. As shown in Fig. 9, almost no infrared signal can be found below 250 °C, which indicates that the composites do not decompose under this temperature. With the temperature increasing, CO, CO_2, and H_2O could be detected. When the temperature increases to 370 °C, a maximum signal intensity at 1,700–1,850 cm^{-1} attributed to carboxylic acid is observed. After that, a maximum signal at 2,800–3,150 cm^{-1} assigned to aliphatic hydrocarbons is observed at the temperature of 480 °C (485 °C for ELDH4). Then, the signal intensity of the pyrolysis products declined gradually, implying that the decomposition of the composites is completed. More detailed information about the pyrolysis products of the composites at different temperatures are shown in Fig. 10.

From Fig. 10a, it can be seen that the release of H_2O from pure EVA shows two steps, the first step begins at about 330 °C and reaches its first peak at about 370 °C. Then, when the temperature is raised to 500 °C, the second step release of H_2O reaches a high level. In the case of flame retardant samples, three steps can be observed in the degradation process of ELDH1 and ELDH4. This correlates well with the TG-DTG results. It is obvious that ELDH1 releases more water than pure EVA below 500 °C. This phenomenon can be illustrated by the following reasons. On one hand, the interlayer structure of LDHs can load lots of water for the composites; on the other hand, –OH groups in LDHs can react with the carboxylic acid formed from the decomposition of the EVA to release more water [36]. When melamine is added into the composites, it is obvious that the release of H_2O is declined significantly. It can be seen that ELDH4 produces less water than ELDH1 in all the process. The reduction of LDHs in the composites may be one reason for this, but the main reason may be the formation of a char layer. The char layer can protect the composites from further burning, thus the decomposition of EVA is slowed down.

As shown in Fig. 10b, no peak can be found in the release of CO_2 for pure EVA until about 500 °C. While a peak attributed to CO_2 can be seen at about 370 °C for both ELDH1 and ELDH4. The peak for ELDH1 may be mainly
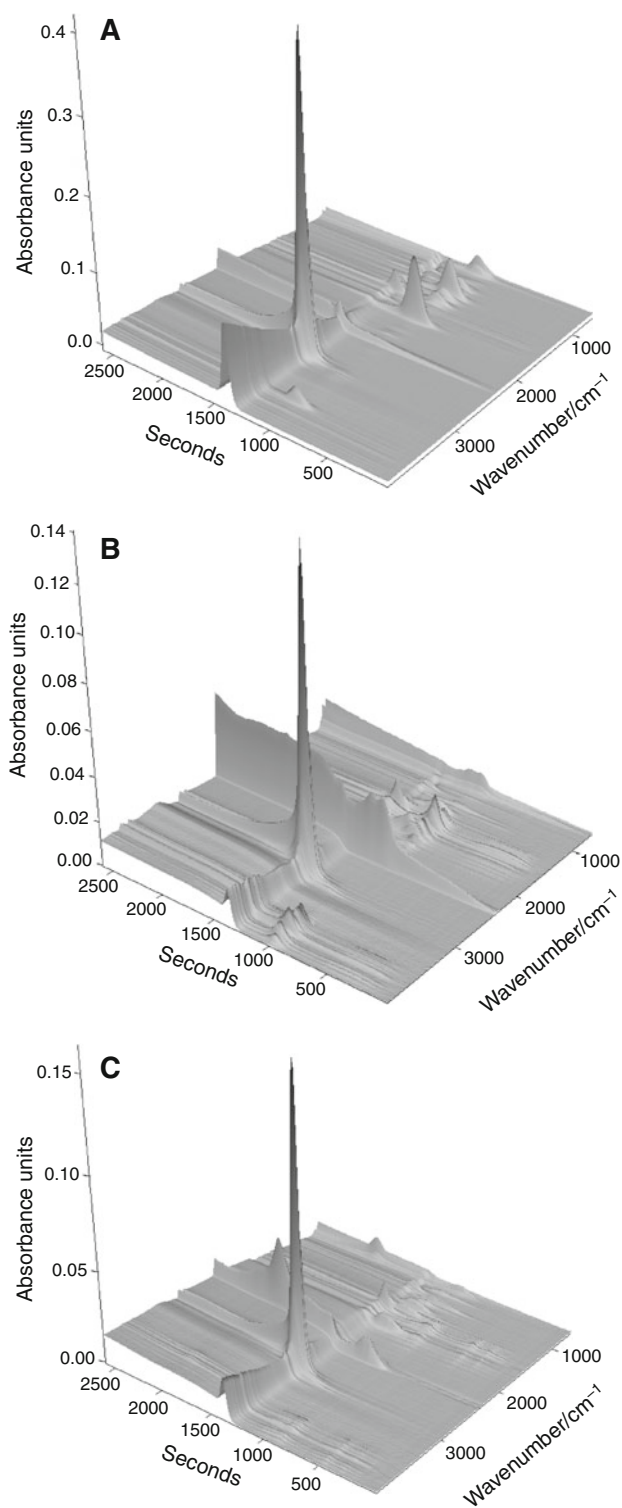
Fig. 8 The 3D TG–IR spectra of pyrolysis products of the composites during the thermal degradation: a EVA, b ELDH1, and c ELDH4

caused by the CO_3^{2-} in LDHs, which can be transformed into CO_2 when heated. For ELDH4, the release of CO_2 is reduced obviously compared with that of ELDH1. The reason may be that with the formation of char on the
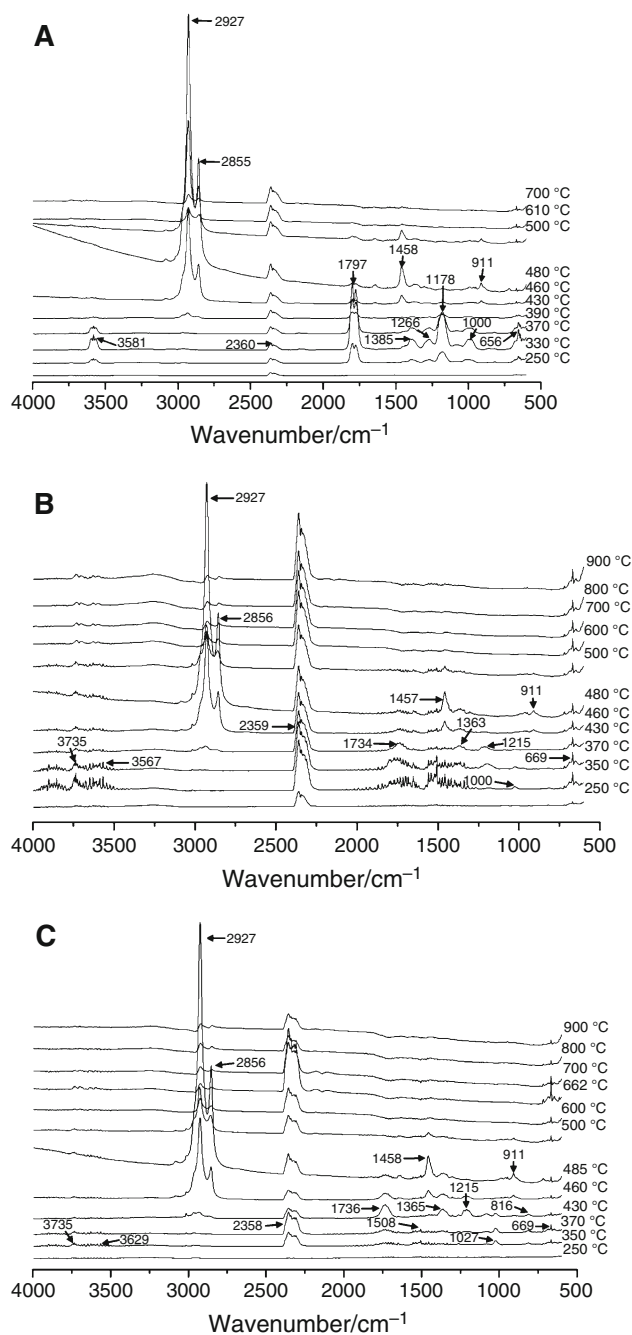

Fig. 9 FTIR spectra of pyrolysis products of the composites at different temperatures: a EVA, b ELDH1, and c ELDH4

surface of the composites, oxygen cannot reach the under layer substrate, thus lots of CO is generated but not CO_2. The peak for ELDH4 at about 700 °C may be illustrated by the holes formed on the char layer.

It is very clear in Fig. 10c that when LDHs is added into EVA, the release of CO is reduced significantly. The decrease of EVA may be one reason for this, but the main reason may be the increase of CO_2. It can also be seen that the ternary composite ELDH4 produces less CO at first, but more afterward compared to that of ELDH1. The reason

Fig. 10 a Changes in the evolved H_2O of the composites cracking in nitrogen at 20 °C min^{-1}. **b** Changes in the evolved CO_2 of the composites cracking in nitrogen at 20 °C min^{-1}. **c** Changes in the evolved CO of the composites cracking in nitrogen at 20 °C min^{-1}. **d** Changes in the evolved carboxylic acid of the composites cracking in nitrogen at 20 °C min^{-1}. **e** Changes in the evolved aliphatic hydrocarbons of the composites cracking in nitrogen at 20 °C min^{-1}
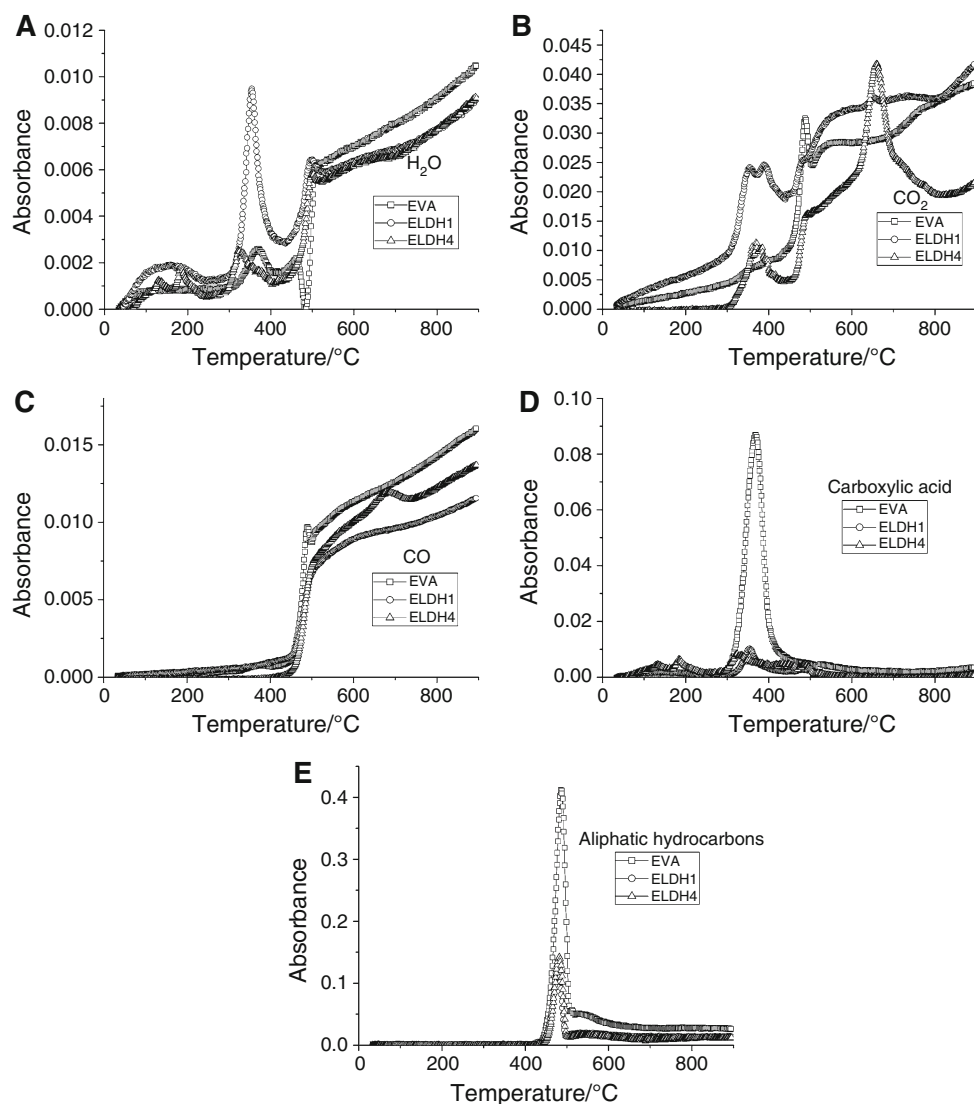
may be that at the temperature of above 500 °C, the formed char layer could be damaged and thus the trapped CO is released out at once.

It can be seen in Fig. 10d that lots of carboxylic acid is evolved from pure EVA, while little can be found for ELDH1 and ELDH4. ELDH1 shows a small peak at the temperature of 350 °C. This may be because LDHs can react with carboxylic acid to form H_2O, thus the release of carboxylic acid is maintained at a low level. When melamine is added into the composites, the amount of LDHs is reduced. So, more carboxylic acid can be released. This is exactly why the release of carboxylic acid for sample ELDH4 shows a slight increase than the ELDH1.

While the evolved carboxylic acid reflects the decarboxylation of EVA, the release of aliphatic hydrocarbons can be used to evaluate the break of the main chain [32]. As shown in Fig. 10e, a sharp peak can be seen for pure EVA. With the addition of LDHs, the release of aliphatic hydrocarbons is decreased significantly. It is interesting to find that when melamine is added into EVA/LDHs composites, the release of aliphatic hydrocarbons is increased slightly. The mechanism of the synergistic effects between melamine and LDHs may be not the gas phase process but the condensed phase process.

Conclusions

Mg/Al/Fe–CO_3 LDHs were synthesized and characterized by XRD and TG. The XRD result showed that the Mg/Al/Fe–CO_3 LDHs were synthesized successfully. The TG–DTG result showed that the interlayer structure of the LDHs can make it load more water than Bayer red mud. It was obvious that the synthesis of LDHs based on Bayer red mud was a promising way for practical use of Bayer red mud.

The flammability characteristics and thermal degradation behavior of EVA/LDHs/melamine composites had been compared with those of EVA and EVA/LDHs by LOI, UL 94, CCT, SDT, and TG–IR analysis. The results showed that melamine had synergistic effects with LDHs when used in EVA. When 5 % melamine was added into the composites, though the LOI value decreased slightly, the composites reached the UL 94 V-0 rating and there was no dripping phenomenon. The CCT data indicated that the HRR of the ELDH4 (containing 5 % melamine) was almost the lowest. The SDT results showed that the composites containing both LDHs and melamine produced less smoke than the EVA/LDHs composites and pure EVA.

It can be seen from TG–IR results that the thermal stability of the EVA/LDHs/melamine composite was improved and the mechanism of the synergistic effects between melamine and LDHs may mainly depend on the condensed phase process.

References

1. Dutta SK, Bhowmick AK, Mukunda PG, Chaki TK. Thermal degradation studies of electron beam cured ethylene–vinyl acetate copolymer. Polym Degrad Stab. 1995;50:75–82.
2. Jiao CM, Chen XL. Synergistic flame retardant effect of cerium oxide in ethylene–vinyl acetate/aluminum hydroxide blends. J Appl Polym Sci. 2010;116:1889–93.
3. Jiao CM, Chen XL. Synergistic effects of titanium dioxide with layered double hydroxides in EVA/LDH composites. Polym Eng Sci. 2011;51:2166–70.
4. Jiao CM, Chen XL. Influence of fumed silica on the flame-retardant properties of ethylene vinyl acetate/aluminum hydroxide composites. J Appl Polym Sci. 2011;120:1285–9.
5. Jiao CM, Wang ZZ, Ye Z, Hu Y, Fan WC. Flame retardation of ethylene-vinyl acetate copolymer using nano magnesium hydroxide and nano hydrotalcite. J Fire Sci. 2006;24:47–64.
6. Ye L, Ding P, Zhang M, Qu BJ. Synergistic effects of exfoliated LDH with some halogen-free flame retardants in LDPE/EVA/HFMH/LDH nanocomposites. J Appl Polym Sci. 2008;107:3694–701.
7. Wang ZZ, Qu BJ, Fan WC, Li Z. Studies on surface modifiers in Mg(OH)₂ flame retarded polyethylene. J Funct Polym. 2001;14:45–8.
8. Zhang M, Ding P, Qu BJ, Guan AG. A new method to prepare flame retardant polymer composites. J Mater Process Technol. 2008;208:342–7.
9. Nyambo C, Kandare E, Wang DY, Wilkie CA. Flame-retarded polystyrene: investigating chemical interactions between ammonium polyphosphate and MgAl layered double hydroxide. Polym Degrad Stab. 2008;93:1656–63.
10. Zhao CX, Liu Y, Wang DY, Wang DL, Wang YZ. Synergistic effect of ammonium polyphosphate and layered double hydroxide on flame retardant properties of poly(vinyl alcohol). Polym Degrad Stab. 2008;93:1323–31.
11. Zhang GB, Ding P, Zhang M, Qu BJ. Synergistic effects of layered double hydroxide with hyperfine magnesium hydroxide in halogen-free flame retardant EVA/HFMH/LDH nanocomposites. Polym Degrad Stab. 2007;92:1715–20.
12. Jiao CM, Wang ZZ, Hu Y. Irradiation crosslinking and halogen-free flame retardation of EVA using hydrotalcite and red phosphorus. Radiat Phys Chem. 2006;75:557–63.
13. Ou YX, Zhao Y, Han TJ, Zhong L. New development of halogen-free flame retarded polycarbonate. Eng Plast Appl. 2009;37:79–83.
14. Liu Y, Wang Q. Study on fire resistance of melt drip of MCA flame retarding nylon 6. Eng Plast Appl. 2005;33:48–50.
15. Liu Y, Wang Q, Hu FY. Studies on modified MCA flame retardant PA6. Polym Mater Sci Eng. 2004;20:220–3.
16. Li D, Hu JP, Qin Y, Sun CM, Wang XY. Combustion behavior and pyrolysis of epoxy resins blended with caged bicyclic dimelamine phosphate. J Funct Polym. 2007;20:81–6.
17. Yang WS, Kim Y, Liu PKT, Sahimi M, Tsotsis TT. A study by in situ techniques of the thermal evolution of the structure of a Mg–Al–CO₃ layered double hydroxide. Chem Eng Sci. 2002;57:2945–53.
18. Huang CB, Zhou RP, Li PY, Lv HJ. The synthesis and characterization of Mg/Al layered double hydroxide (LDH). Anhui Chem Ind. 2009;35:21–4.
19. Zanetti M, Kashiwagi T, Falqui L, Camino G. Cone calorimeter combustion and gasification studies of polymer layered silicate nanocomposites. Chem Mater. 2002;14:881–7.
20. Jiao CM, Chen XL. Synergistic effects of zinc oxide with layered double hydroxides in EVA/LDH composites. J Therm Anal Calorim. 2009;98:813–8.
21. Hirschler MM. In: Heat Release in Fires. London: Elsevier; 1992. p. 375–422.
22. Kuzawa K, Jung YJ, Kiso Y, Yamada T, Nagai M, Lee TG. Phosphate removal and recovery with a synthetic hydrotalcite as an adsorbent. Chemosphere. 2006;62:45–52.
23. Xie RC, Qu BJ. Synergistic effects of expandable graphite with some halogen-free flame retardants in polyolefin blends. Polym Degrad Stab. 2001;71:375–80.
24. Grexa O, Lubke H. Flammability parameters of wood tested on a cone calorimeter. Polym Degrad Stab. 2001;74:427–32.
25. Fu MZ, Qu BJ. Synergistic flame retardant mechanism of fumed silica in ethylene-vinyl acetate/magnesium hydroxide blends. Polym Degrad Stab. 2004;85:633–9.
26. Shi L, Li DQ, Li SF, Wang JR, Evans DG, Duan X. The Structure, flame retarding and smoke suppressing properties of Zn-Mg-Al-CO₃ layered double hydroxides. Chin Sci Bull. 2005;50:1101–4.
27. Shukri TM, Mosnacek J, Basfar AA, Bahattab MA, Noireaux P, Courdreuse A. Flammability of blends of low-density polyethylene and ethylene vinyl acetate crosslinked by both dicumyl peroxide and ionizing radiation for wire and cable applications. J Appl Polym Sci. 2008;109:167–73.
28. Hirose S, Kobashigawa K, Izuta Y, Hatakeyama H. Thermal degradation of polyurethanes containing lignin studied by TG-IR. Polym Int. 1998;47:247–56.
29. Salgado J, Paz-Andrade MI. The effect of firesorb as a fire retardant on the thermal properties of a heated soil. J Therm Anal Calorim. 2009;95:837–42.
30. Costache MC, Jiang DD, Wilkie CA. Thermal degradation of ethylene-vinyl acetate copolymer nanocomposites. Polymer. 2005;46:6947–58.
31. Gao M, Wu W, Yan Y. Thermal degradation and flame retardancy of epoxy resins containing intumescent flame retardant. J Therm Anal Calorim. 2009;95:605–8.
32. Gregoriou VG, Kandilioti G, Bollas ST. Chain conformational transformations in syndiotactic polypropylene/layered silicate nanocomposites during mechanical elongation and thermal treatment. Polymer. 2005;46:11340–50.

33. Weil ED, Pate NG. Iron compounds in non-halogen flame-retardant polyamide systems. Polym Degrad Stab. 2003;82: 291–6.

34. Chen YJ, Zhan J, Zhang P, Nie SB, Lu HD, Song L, Hu Y. Preparation of intumescent flame retardant poly(butylene succinate) using fumed silica as synergistic agent. Ind Eng Chem Res. 2010;49:8200–8.

35. Polli H, Pontes LAM, Souza MJB, Fernandes VJ Jr, Araujo AS. Thermal analysis kinetics applied to flame retardant polycarbonate. J Therm Anal Calorim. 2006;86:469–73.

36. Nie SB, Zhang MX, Yuan SJ, Dai GL, Hong NN, Song L, Hu Y, Liu XL. Thermal and flame retardant properties of novel intumescent flame retardant low-density polyethylene (LDPE) composites. J Therm Anal Calorim. 2012;109:999–1004.